Review article

M. Munzer Alseed, Sajjad Rahmani Dabbagh, Peng Zhao, Oguzhan Ozcan and Savas Tasoglu*

Portable magnetic levitation technologies

https://doi.org/10.1515/aot-2021-0010
Received February 16, 2021; accepted April 19, 2021;
published online May 10, 2021

Abstract: Magnetic levitation (MagLev) is a density-based method which uses magnets and a paramagnetic medium to suspend multiple objects simultaneously as a result of an equilibrium between gravitational, buoyancy, and magnetic forces acting on the particle. Early MagLev setups were bulky with a need for optical or fluorescence microscopes for imaging, confining portability, and accessibility. Here, we review design criteria and the most recent end-applications of portable smartphone-based and self-contained MagLev setups for density-based sorting and analysis of microparticles. Additionally, we review the most recent end applications of those setups, including disease diagnosis, cell sorting and characterization, protein detection, and point-of-care testing.

Keywords: low-cost; magnetic levitation; optics; smartphone diagnostic.

***Corresponding author: Savas Tasoglu**, Boğaziçi Institute of Biomedical Engineering, Boğaziçi University, Çengelköy, 34684 Istanbul, Turkey; Department of Mechanical Engineering, Koç University, Sariyer, 34450 Istanbul, Turkey; Koç University Arçelik Research Center for Creative Industries (KUAR), Koç University, Sariyer, 34450 Istanbul, Turkey; Koc University Research Center for Translational Medicine, Koç University, Sariyer, 34450 Istanbul, Turkey; and Center for Life Sciences and Technologies, Bogazici University, Bebek, 34342 Istanbul, Turkey,
E-mail: stasoglu@ku.edu.tr
M. Munzer Alseed, Boğaziçi Institute of Biomedical Engineering, Boğaziçi University, Çengelköy, 34684 Istanbul, Turkey
Sajjad Rahmani Dabbagh, Department of Mechanical Engineering, Koç University, Sariyer, 34450 Istanbul, Turkey; and Koç University Arçelik Research Center for Creative Industries (KUAR), Koç University, Sariyer, 34450 Istanbul, Turkey
Peng Zhao, The State Key Laboratory of Fluid Power and Mechatronic Systems, College of Mechanical Engineering, The Key Laboratory of 3D Printing Process and Equipment of Zhejiang Province, College of Mechanical Engineering, Zhejiang University, 310027 Hangzhou, China. https://orcid.org/0000-0002-3815-1248
Oguzhan Ozcan, Koç University Arçelik Research Center for Creative Industries (KUAR), Koç University, Sariyer, 34450 Istanbul, Turkey

1 Introduction

Among the techniques used for controlling the position of micro-objects, magnetophoresis-based manipulation offers various advantages including contactless, low-cost, and power-free manipulation of micro-objects such as live cells and functionalized plastic beads. Several applications were demonstrated in the literature by applying magnetic fields for various liquid biopsies such as blood [1], urine [2], and tear [3] utilizing various fluidic states such as static-fluid-setting [4], Poiseuille-flow cases [5, 6], and inertial focusing [7, 8]. An emerging theme of using low-cost magnetics is magnetic levitation (MagLev) where the particle sorting is achieved mainly through the utilization of two permanent magnets in anti-Helmholtz configuration (i.e., like poles facing) [9, 10]. MagLev relies on the fact that the difference in density between the suspended object and suspending medium directly affects the levitation height of levitated particles [11–15]. In other words, the average levitation height is directly correlated to either the objects' or solution's densities, enabling the density measurement of both by varying one while keeping the other constant. Levitation height is independent of the particle shape, size, chemical composition, and mechanical properties such as viscosity, elasticity, and stiffness. MagLev requires minimal sample preparation and can separate different materials with various densities simultaneously.

MagLev has two distinct applications: first, suspension of bearings, flywheels, and vehicles (e.g., trains) and propulsion of them using magnets [16, 17]; second, suspension of diamagnetic materials (solids, pastes, gels, liquids, heterogeneous materials, colloidal suspensions, and organic matter – all organic matter is diamagnetic, except stable free radicals) in a paramagnetic medium (which supplies magnetic and buoyant forces) [18, 19]. Initially, MagLev was used to levitate strongly diamagnetic material (e.g., pyrolytic graphite and bismuth) in the air using an electromagnetic field (1939) [20]. By the end of the 1960s, MagLev found applications in the production of frictionless rotors (1966) [21], tiltmeter (1968) [22], and accelerometers (1969) [23], followed by separation of plastic, metals, and minerals in 1970s (1976) [24]. Subsequently, the use of resistive solenoid electromagnets and superconducting, in the 1990s, living organisms, wood, water, glass, and

ethanol were levitated by MagLev [18, 25–27]. Latterly, the emergence of neodymium iron boron (NdFeB) permanent magnets, in 1984, which eliminated the need for bulky, complex, and costly electromagnets, has extended the application of MagLev to miniaturized point-of-need applications [28, 29]. The first studies in the field of MagLev were performed via direct measurement of levitation height using a ruler since the setups used to be relatively large, requiring the use of strong magnets with dimensions of $5 \times 5 \times 2.5$ cm in order to have enough magnetic force [13, 30, 31]. Determination of nutrition content of food products (e.g., dairy) [32], analyzing forensics evidence in tiny particles [33], characterizing polymer composition [34] and crystal polymorphs [35], tracking the dynamics of chemical reactions, quantifying protein binding degree [36], and more recently measuring antigen-antibodies binding in quantitative immunoassays [37] are a number of applications of large MagLev setups. In addition, the ability of MagLev to manipulate, align, and assemble easily damageable objects (e.g., soft/fragile submillimeter objects) has also been utilized to guide self-assembly processes by altering the magnetic field to change the position and orientation of objects without physical contact [18, 30, 38]. In order to augment the clinical and commercial impact of MagLev, these devices need to become more reliable, robust, portable, cost-effective, and available in the point of need.

Levitating objects in smaller setups results in more portable devices, leads to a higher reliability by lowering the chance of interference with surrounding electronics, decreases the amount of needed reagents which ultimately minimizes the cost of each test, increases the robustness by reducing the required time for equilibrium, and empowers setups to levitate and analyze micron size particles (e.g., biological samples) [39]. In this regard, smaller magnets have been reported with dimensions of $2 \times 5 \times 50$ mm [12]. Availability of a biocompatible paramagnetic medium (e.g., Gd chelates) and being able to levitate micron size objects make MagLev a suitable method for separation and analysis of cells, viruses, or bacteria from normal cells [40], tracking the growth of cells, analysis of pathophysiological changes associated with genetic disorders or infections [41], and analysis of blood and kidney function [18, 42, 43]. In order to be able to analyze and manipulate submillimeter samples, an imaging system such as an optical or fluorescence microscope is required, increasing the overall cost of the device, necessitating expert technicians to perform the test, and confining the portability [39, 44]. Ever improving computational power and image acquisition capabilities of smartphones as well as the ubiquity of them has provided a potential platform to be integrated with MagLev setups [39, 44]. Smartphone-based MagLevs offer a low-cost and portable device with no need for an external power source to levitate objects.

In this paper, decisive design parameters of MagLev setups, advantages, and pitfalls of each category (large, smartphone-based, and self-contained MagLevs) are reviewed. Moreover, we review the end applications of smartphone-based and self-contained MagLev setups, such as label-free cell separation [45], blood analysis [46, 47] such as quantification of changes in red blood cell (RBC) density for sickle cell diagnosis [44], disease diagnosis (e.g., hepatitis C [10]), magnetic focusing [48], and tumor detection [45].

2 Magnetic levitation platforms: design perspective

Three main constituents of a MagLev setup, that should be considered during the design process to satisfy proposed needs, are magnets, paramagnetic medium, and imaging equipment.

Magnets: Magnets are the source of the magnetic field in MagLev setups. While the use of electromagnets [49] and permanent rare-earth magnets (e.g., NdFeB) [44] has been reported in the literature, permanent magnets are of higher interest in MagLev applications since no external power source is needed to levitate objects [18, 30]. Decisive features of magnets to be considered in design and magnet selection are: (i) material and size of magnets should be chosen so that magnets can provide enough force to be able to suspend objects depending on the mass of objects, the distance of two magnets from each other, and magnetic properties of the paramagnetic medium; (ii) magnets should provide a permanent and consistent magnetic field during the levitation time; (iii) magnets should have high coercivity H_c, which means high resistance to being demagnetized by external magnetic fields [18]; and (iv) magnets should preferably be cost-effective and commercially available. Furthermore, MagLevs with various magnet geometries are reported, such as ring-shaped [50] and cubic magnets [44]. Most commonly, MagLev uses two magnets with like-poles-facing in which the magnetic field is maximum near magnets and diminishes to virtually zero (in the case of using identical magnets) at the center of the gap between two magnets [39]. This configuration of magnets can produce a linear magnetic field, simplifying measurement and calibration of setup. Nonlinear magnetic fields are also useful mostly for separation purposes that only relative density is of interest [18]. One of the main

limitations of MagLev is that magnetic force is applied to all objects concomitantly, with no possibility of exerting varying magnetic force to one of the levitated objects independent of other objects [30].

Paramagnetic medium: The paramagnetic medium exerts a buoyant force (proportional to the density difference between the sample and the medium) as well as magnetic force (proportional to the difference in magnetic susceptibility between the sample and the medium) on particles, facilitating the levitation of objects [18]. Applying a magnetic field exerts a magnetic force (which can be aligned to be parallel with gravitational force) on the particles, levitating them in a certain height proportional to their density. Particles with lower density levitate at higher heights compared to denser ones, facilitating the separation of particles with different densities simultaneously [51]. A higher concentration of the paramagnetic medium not only results in a wider range of detectable densities (wider dynamic range of detection) as a consequence of stronger magnetic forces exerted by the medium but also shifts equilibrium height near the centerline and shortens equilibrium time [52]. Conversely, a lower concentration of the paramagnetic medium eventuates in improving the ability of setup to distinguish smaller density differences between particles (better resolution of detection) while particles levitate away from the centerline [39]. Different families of paramagnetic material have been reported in the literature with different characteristics, such as (i) aqueous solutions paramagnetic salts (e.g., solutions of $GdCl_3$ or $MnCl_2$) that are suitable for water-insoluble samples, (ii) aqueous solutions of biocompatible chelates of Mn^{II} and Gd^{III} are useful for biological applications (e.g., cellular and protein assays), (iii) nonaqueous solutions of salts, $MnCl_2$, and $GdCl_3$ (soluble in alcohols) that are less dense than water, and therefore are useful to suspend object less dense than water (e.g., polypropylene and polyethylene), (iv) paramagnetic ionic liquids that have low melting points, negligible vapor pressures, and high thermal stabilities, and (v) phase-separated paramagnetic media [18, 31, 36, 53–55].

Imaging method: In conventional MagLev setups, owing to the large size of the magnets and levitating chamber, levitated objects can be detected by the naked eye for manual measurement of density using a ruler [56]. The development of smaller setups for submillimeter measurements necessitates the use of more advanced imaging techniques. Optical/fluorescent microscopy is a promising method to image-levitated microparticles for later analysis either by human experts or computers. However, requiring experts to use the microscope, the large size as well as the high cost of microscopes, and demanding external power source pose challenges regarding portability and affordability of microscopy-based MagLev setups in resource-limited settings [51]. On the other hand, the superior image acquisition and computational power of smartphones offer an unprecedented opportunity to extend the applications of MagLev devices. Although, compared to microscopes, smartphone cameras do not normally have a high numerical aperture (NA) which is essential for high-resolution imaging of submillimeter objects, using an external lens and light-emitting diodes (LEDs) can empower smartphones to acquire images of cells and bacteria [44, 51]. Hence, MagLev systems integrated with smartphones are more portable, affordable, user-friendly, and demands no external power compared to microscope-based MagLev setups [10]. However, standardization of setups for various smartphones, with different operating systems and camera properties, may pose challenges for designers and clinicians [52]. Self-contained MagLev setups use a separate camera, instead of a smartphone, for image acquisition, addressing the possible predicaments of magnetic interference between smartphone and setup [52, 57] as well as adapting different smartphones to a MagLev setup [52, 57]. However, self-contained devices need an external controller board and image storage. Important features of each setup are summarized in Table 1.

3 Emerging end-applications of portable magnetic levitation setups

3.1 Smartphone-based MagLev setups

The advantages of smartphone-based MagLev, including portability, user-friendliness, and low cost, make it especially suitable for point-of-care applications, such as micro-object (e.g., cell) sorting in resource-limited regions [51].

3.1.1 Sortation, quantification, and characterization of micro-objects

Separation of micro-objects with a smartphone was done by a study in which a low weight (62 g) customized attachment was designed, 3D-printed, and installed over a smartphone (Figure 1a) [39]. The attachment utilized a magnification lens (with an outer diameter of 6.33 mm, a numerical aperture of 0.64 mm, and an effective focal length of 4.03 mm) positioned between the smartphone's

Table 1: Comparison of the main characteristics of common MagLev setups.

	Large-Maglev	Smartphone-Based	Self-Contained
Magnet sizes	Relatively large (50 × 50 × 25 mm)	Small (50 × 2 × 5 mm)	Small (50 × 2 × 5 mm)
Advantages	– Useful to measure densities of relatively large objects. – Direct measurement of levitation height using a ruler with no need for external readers (e.g., microscopes). – Short time to reach equilibrium.	– Portable. – Low-cost (excluding the smartphone, ~$100) – Suitable for point-of-care settings. – Useful to measure densities of micro-objects, such as cells and yeasts. – User-friendly.	– Portable. – Low-cost for the whole setup (<$100). – Suitable for point-of-care settings. – Useful to measure densities of micro-objects. – Standardized and user-friendly.
Disadvantages	– Limited portability. – Costly due to the use of larger magnets and more paramagnetic medium. – Magnetic field can be affected by interference with external fields.	– Relatively long time to reach equilibrium. – Standardization (since different smartphones with different operating systems and camera setups are available in the market). – Sample density can be affected by the heat generated by the LED and smartphone. – Possibility of interference of magnetic/electric field of the smartphone with MagLev setup.	– Relatively long time to reach equilibrium (10–15 min). – Sample density can be affected by the heat generated by the LED.
Optics	No optics. Measurement is performed directly by the naked eye using a ruler.	Smartphone camera, magnifying lens, light diffuser, LED, and emission filters.	Low-cost camera, an adjustable magnifying lens with a focus ring, light diffuser, LED.
References	[32–35, 56, 58]	[39, 44–48, 51]	[52, 57]

camera and a microcapillary (0.98 mm by 0.98 mm square tube), through which micro-objects of different densities were suspended in a paramagnetic medium (Gadolinium-based (Gd+)). The captured images were then analyzed using a custom Android application installed on the same smartphone to measure the levitation height and calculate an estimation of the densities accordingly. Additionally, two aspects were characterized: imaging capabilities (sharpness of obtained images) and the effect of thermal flux from the smartphone's screen and the illumination LED. Analysis of imaging capabilities showed an inverse linear correlation between the sharpness of microspheres and their distance from the center (i.e., as the distance from the centerline increases, the sharpness decreases). Thermal quantification showed that heat generated by the smartphone did not considerably affect the temperature of the fluid in the capillary tube, and therefore density estimation. It was demonstrated that a higher concentration of the paramagnetic medium reduces the equilibrium time (less than 1 min for the highest concentration) and causes the particles to reach an equilibrium height close to the centerline (Figure 1c, d). According to Figure 1e, the density of microspheres was inversely correlated to their levitation height (i.e., denser particles levitate close to the centerline). Besides, a lower concentration of the paramagnetic medium can provide better detection resolution, empowering setup to detect subtle density differences (Figure 1e). Moreover, it was shown that larger microspheres reach equilibrium height faster than smaller microspheres, whereas the particle size did not affect the levitation height substantially (Figure 1f) [39].

Another study aimed to provide an effective 3D-printed smartphone-based, low-cost, and portable MagLev device for real-time monitoring, sorting, and quantification of micro-objects in a flowing fluid, which has special importance for biomedical applications such as real-time analysis of drug [45]. Three different 3D-printing techniques were used to evaluate multiple printing metrics, including cost, printing time, and resolution. The device was 3D-printed using Objet30 prime Polyjet 3D printer, Formlabs 2 stereolithography (SLA) 3D printer, and MakerBot Replicator fused deposition modeling (FDM) 3D printer (the working principle of these 3D printing techniques is available elsewhere [59, 60]). To assess printing metrics, five parts of the device

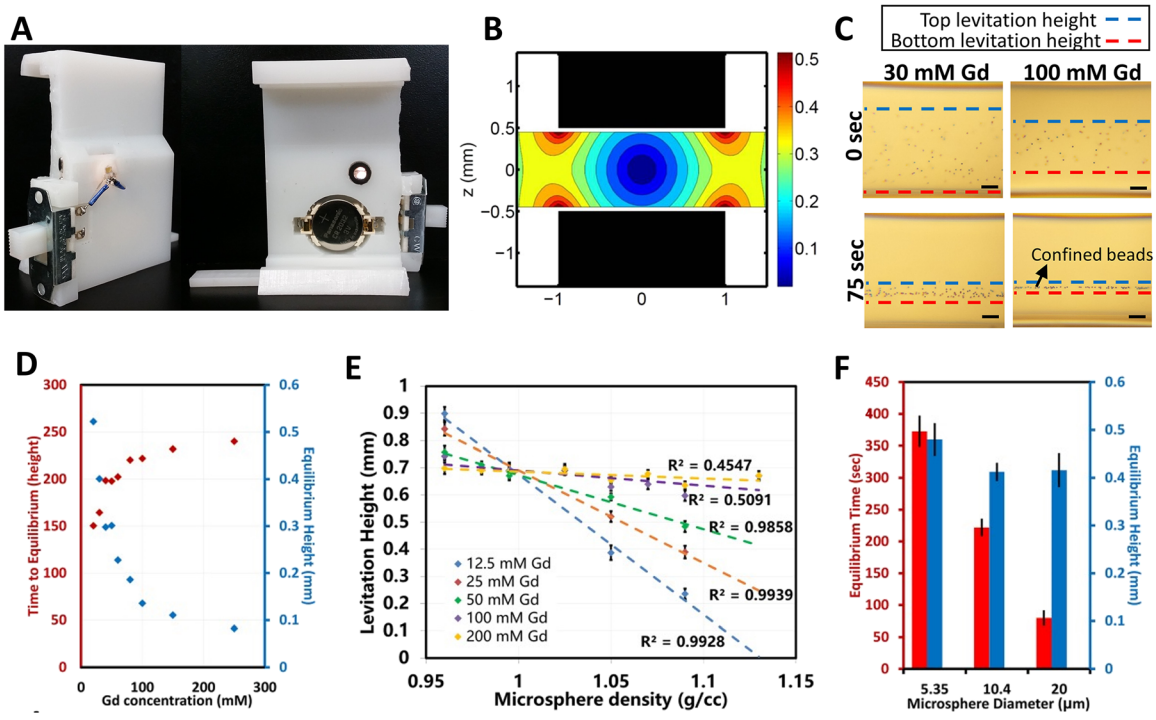

Figure 1: Smartphone-attachable MagLev setup for density-based separation of particles.
(a) View of the 3D-printed case. (b) Magnetic field lines displaying the magnetic field between the two magnets. (c) Focusing of 10 μm polystyrene microspheres in 30 and 100 mM solution over 0, 15, and 75 s of being placed between magnets. Dashed lines demonstrate bottom (red) and top (blue) confinement limits. (d) Effects of concentration of the paramagnetic medium on the equilibrium time (red) and height (blue). (e) Correlation of density of particles and levitation height obtained by levitating eight microspheres with standard density. Dashed lines present different concentrations of the paramagnetic medium, highlighting better detection resolution of the medium with lower concentration. (f) Influence of microsphere size on the equilibrium height (blue) and time (red). As illustrated, while larger particles reach equilibrium faster, the size of microparticles had no considerable effect on the levitation height [39]. The size of the magnets was $5 \times 0.2 \times 0.5$ cm and the size of the encasement of the smartphone-attachable MagLev setup was approximately $7.9 \times 5.3 \times 2.8$ cm. Scale bars are 100 μm.

were printed using the three 3D printing methods. All parts printed with the polyjet printer were working properly, compared to only two parts for the FDM, and four parts for the SLA printer. However, printing using the polyjet printer costed 30-times more than an FDM printer and four-times more than an SLA printer. Printing time was not significantly different among different combinations of parts, ranging from 25.2 to 28.7 h. Therefore, an optimized combination of the five parts was chosen based on the cost analysis. In terms of resolution, parts printed with the polyjet printer showed the best accuracy and precision [45]. After printing, the device was used with the same setup, which was a mixture of different blood cells and cancer cells, suspended in a paramagnetic solution that flows through a magnetic field. Figure 2d illustrates the end applications of the proposed device for cancer cell sorting. The MagLev setup successfully separated breast, lung, prostate, and ovarian cancer cells from blood cells with distinct confinement lines.

In another study (similar setup to [45]), smartphone attachment was 3D-printed, and a magnifying lens was placed on the smartphone's camera, while a microcapillary was placed between the lens (numerical aperture of 0.64 mm and diameter of 6.33 mm) and illumination LED (Figure 3a) [48]. Diamagnetic particles with the gadolinium-based paramagnetic solution were pumped into the capillary which was surrounded by two permeant NdFeB magnets ($50.8 \times 2 \times 5$ mm^3). The device utilized the flow of the sample and the magnetic field to keep micro-objects suspended at their equilibrium height, determined by the density of each particle. The smartphone's camera was used to acquire images of the suspended objects, and a custom Android application was used to process the images to show that particles were successfully sorted based on their densities. The study also investigated the effects of magnet size and flow rate on the sorting performance of micro-objects. In this regard, the previous experiment was

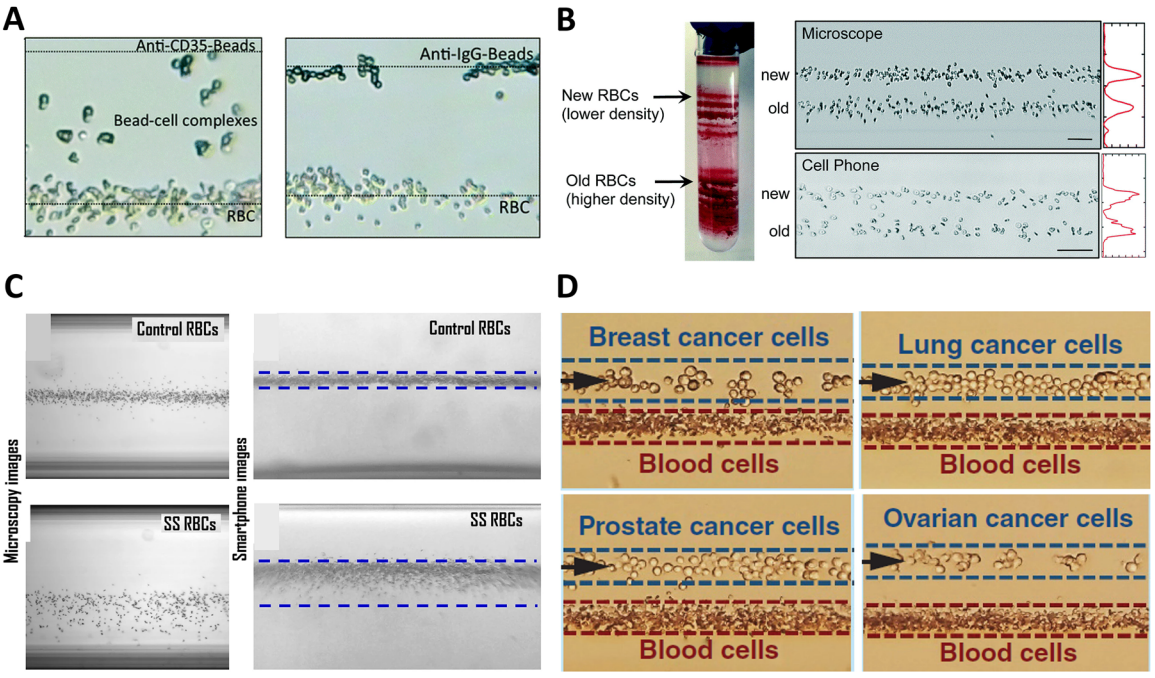

Figure 2: End applications of smartphone-based MagLev setups.
(a) Detection of membrane-bound and soluble antigens. A smartphone image of anti-CR1 antibody-coated bead and RBC complexes from a high CR1 expresser [61]. (b) (Left) centrifugation was used to separate RBCs of different ages in Percoll gradient solution. (Right) old and new RBCs levitated in two bands based on density. Red graphs indicate the intensity profiles. All scale bars represent 50 μm [47]. (c) Sickle cell separation performance of the microscopy-based method (left) and smartphone-based MagLev (right). The top images show controlled RBCs, where the bottom images are SS RBC (sickle cell anemia (SS genotype)) with higher density [44]. (d) Confinement of breast, lung, prostate, and ovarian cancer cells, together with blood cells, manifesting high separation efficiency and image acquisition quality of smartphone-based MagLev devices [45]. The size of the magnets was 5 × 0.2 × 0.5 cm and the size of the encasement of the smartphone-attachable MagLev setup was approximately 7.9 × 5.3 × 2.8 cm.

conducted with magnets of different lengths, ranging from 10 to 50 mm. Additionally, three different flow rates were used to pump the solution, namely 0.1, 0.25, and 0.75 μL s^{-1} (Figure 3b, c). The results showed that either increasing the magnet length or decreasing flow rate eventuates in increasing the accuracy of particle separation (i.e., less scattering of microparticles from the equilibrium line). This can be explained by the fact that the shorter magnets or faster flow rates decrease the exposure of particles to the magnetic field, giving them less time to focus and reach an equilibrium [48].

3.1.2 Diseases diagnosis and cell sorting

Membrane-bound and soluble antigens, found in blood, were detected using a smartphone-based MagLev setup, which can be used to detect infectious diseases such as HIV, HAV, HBV s.a, EBV, Dengue, Zika, and Chikungunya (Figure 2a) [61]. T-cell antigen CD3, RBC antigens CD35 and RhD, eosinophil antigen Siglec-8, soluble IL-6, and RBC-bound Epstein–Barr viral particles were successfully detected by the proposed setup. The detection performance was validated with immunofluorescence microscopy. This MagLev setup was potent enough to be used as a replacement for enzyme-linked immunosorbent assay (ELISA), flow cytometry, or microscopy for the detection, screening, and quantification of various blood pathogens and antigens in resource-limited settings [61]. In another study, a smartphone-based MagLev setup was used to detect and sort cells in 15 min [47]. In order to verify the performance of the setup, RBCs with artificially altered densities, and reference beads, with known densities, were used. A microscope was also used to take the images to be compared with smartphone images. To demonstrate an example application of the device, RBCs were taken from healthy individuals and anemia patients, and the resulted images showed that anemic cells had higher levitation height due to their lower densities compared to healthy RBCs. Furthermore, separation of old and fresh RBCs was successfully performed with the platform, showing that old RBCs have more density than fresh ones (Figure 2b). Comparison of microscope results

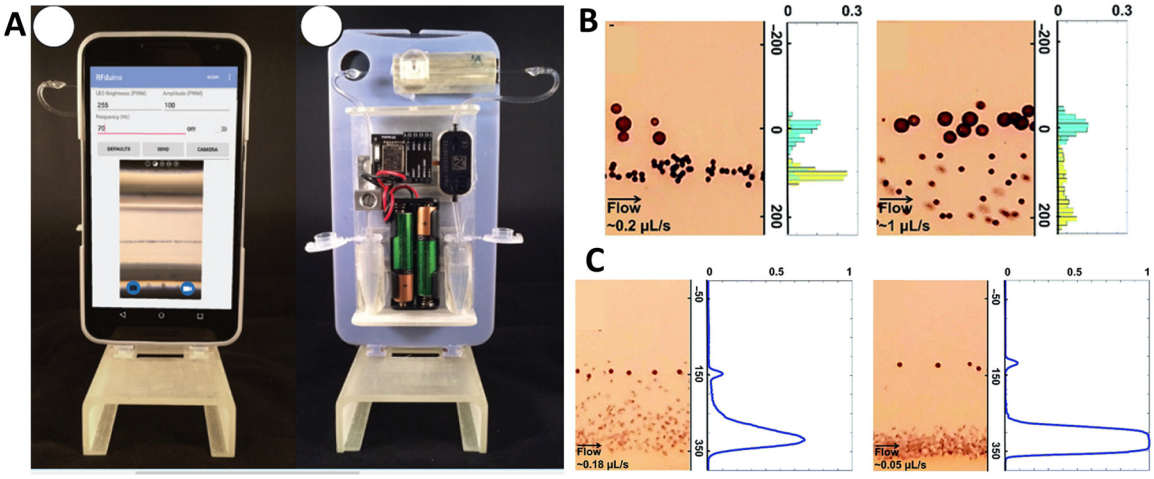

Figure 3: Flow-assisted MagLev setup.
(a) A smartphone-based MagLev setup which was able to levitate and image particles while flowing. This setup enabled real-time analysis of samples. (b) Separation of blood cells and particles at low (0.2 µL s^{-1}) and high (1 µL s^{-1}) flow rate. Blue and green histograms represent microspheres with densities of 0.97 and 1.12 g cm^{-3}, respectively. (c) Summed and normalized pixel intensities of microparticles and blood cells flowed at 0.18 and 0.05 µL s^{-1}. Relatively low numbers of microspheres compared to blood cells elucidate the rare particle detection and sorting capability [48].

and smartphone images demonstrated a comparable performance [47].

Sickle cell diseases can be a severe life-threatening illness if left undiagnosed. A 3D-printed smartphone attachment, similar to the setup in [39], was developed to measure the difference in levitation height of blood cells in a small blood sample, aiming to separate sickle blood cells which have higher density compared to normal cells [44]. The proposed setup was portable with minimal need for sample preparation (e.g., no centrifugal sample preparation). As an addition to the previous setup, a microscope-compatible capillary holder was fabricated to compare results with the MagLev outcome. After capturing images of the sickle RBCs and control blood cells, the separation was accomplished, reporting that control RBCs had higher levitation height and distributed within a narrow area, while sickle cells levitated at lower heights and distributed in a wider range (Figure 2c). Microscope images substantiated the ability of the proposed smartphone-based MagLev setup for the analysis of sickle cells [44]. Although the setup was able to perform label-free detection of single cells with the aid of digital image processing, it was a static setup unable to monitor real-time responses of cells to stimuli (e.g., real-time monitor of influences of a certain drug on a particular type of cells).

As another end application of smartphone-assisted MagLev, a setup was developed to detect Hepatitis C (HCV) using micro-sensor beads (MS beads), which were functionalized by anti-HCV NS3 antibody [10]. The proposed setup comprised four mirrors, no magnification optical lens, NdFeB magnets (50.8 × 6.35 × 3.175 mm), a capillary channel (1 × 1 mm cross-section, 50 mm length), and LED. The setup was firstly optimized by density marker polyethylene beads. Subsequently, visualizing MS beads with a smartphone camera, without an external lens, objects (HCV NS3 protein) as small as 45–53 µm was detectable in 30 µL of the sample with a detection limit of 50 µg mL^{-1}, which was 10 times better than conventional ELISA [10] (Figure 4a).

Another smartphone-based MagLev imaging device, known as i-LEV, was developed for label-free separation, identification, and counting of white blood cells (WBCs) and RBCs mixed together in a paramagnetic medium, ultimately to facilitate point-of-care diagnostics [46]. The devicecomprised a front panel to hold system components, a lens that focuses the sample's image onto the smartphone's camera, a set of NdFeB permeant magnets (50 mm length, 5 mm height, and 2 mm width), mirrors, capillary channels (50 mm length, 0.2 mm wall thickness, and 1 × 1 mm cross-section), LEDs that illuminate the sample, and filters that enhance the obtained images. The proposed setup was compatible with different smartphones. To perform cell separation, the smartphone's camera was aligned with the lens, while two mirrors were used to reflect the light from the LED to illuminate the sample. Microscopy was also used to image the samples and confirm the validity of i-LEV (Figure 4b). The same experiment was

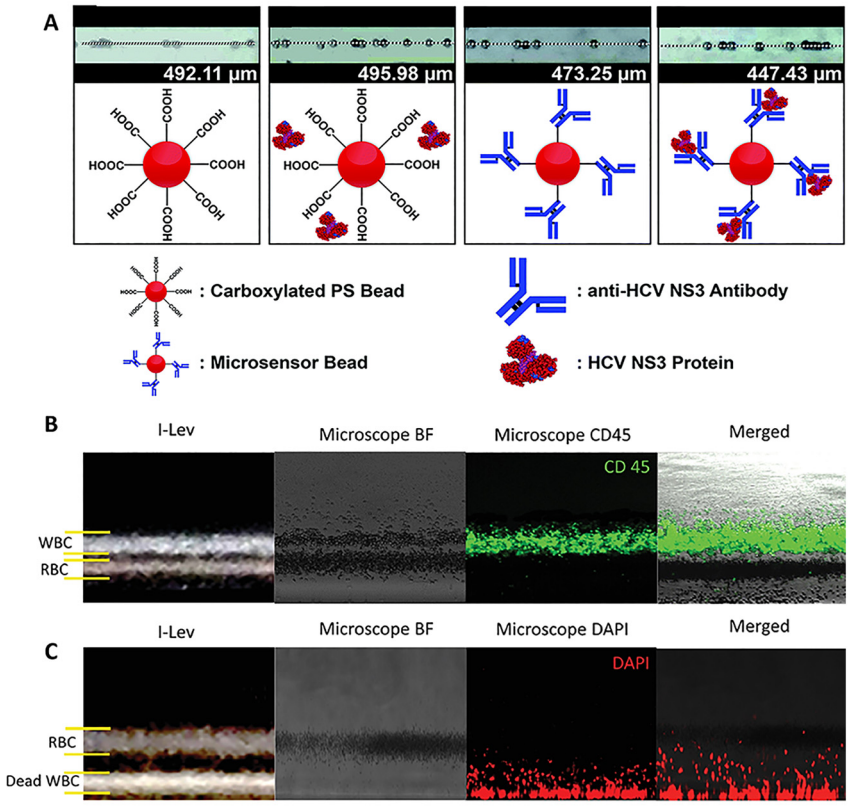

Figure 4: Smartphone-assisted platforms.
(a) Levitation heights for polystyrene beads for hepatitis C detection. From left to right, nonfunctionalized PS beads in the absence of HCV NS3 protein solution, nonfunctionalized PS beads in the presence of HCV NS3 protein solution, MS beads in the absence of HCV NS3 protein solution, and MS beads in the presence of HCV NS3 protein solution. The smartphone-assisted MagLev setupcomprised magnets with the size of $5 \times 0.2 \times 0.5$ cm, and a box with approximate size of $13.5 \times 32 \times 20$ cm [10]. (b, c) Integrating cell phone imaging with magnetic levitation (i-LEV) for label-free blood analysis. (b) Images of WBC and RBC taken by i-LEV and microscope (bright field, fluorescent images of CD45-labeled WBC, and overlap of the bright field and CD45 images). (c) Live–dead assay imaging of RBCs and WBCs by i-LEV and microscope (bright field, 4′,6-diamidino-2 phenylindole dihydrochloride (DAPI) labeled, and overlapping images). Live RBCs levitated while dead WBCs sedimented at bottom of the capillaries [46].

successfully performed to separate dead WBCs from RBCs based on their density (Figure 4c). i-LEV was also used to quantify RBCs using phosphate buffered saline (PBS) as a medium of suspension, demonstrating that PBS with a higher concentration of blood cells takes more time to reach equilibrium. It was also shown that there was a positive linear correlation between the concentration of blood cells and the bandwidth of levitated blood in the channel for both RBCs, in the range of 50–250 mL^{-1}, and WBCs [46].

Smartphone-based MagLev was integrated with fluorescence microscopy, allowing density-based sortation of cells to determine cell type, their activity, and image them in three imaging modes, bright field, darkfield, and fluorescent [51]. The device comprised a custom 3D-printed case for the smartphone that also allows attaching other components, including a capillary tube, an aspheric lens with a numerical aperture of 0.64 mm and a diameter of 6.33 mm, two focusing N52-grade nickel-plated NdFeB magnets ($50.8 \times 2 \times 5$ mm^3), colored LEDs, emission filters for bright field and dark field modes, and electronical components to exchange emission filters (Figure 5a–c). The entire case and equipment, smartphone excluded, weighted 214 g. The overall cost of the device was $105.87. To assess the abilities of the device, microspheres of different sizes (ranging from 5.35 to 79 µm) were mixed with 100 mM gadolinium-based paramagnetic solution, loaded into a microcapillary tube, held between a pair of magnets, and shined with a warm white LED. The smartphone's camera then captured the light traveled through the sample with the aspheric lens in both brightfield and darkfield modes. A MATrix LABoratory (MATLAB) code was used to identify the sizes of microspheres and compare the image quality of both microscopy modes. For fluorescence

imaging, red, green, and blue fluorescent microspheres were used, along with white, blue, and ultraviolet (UV) LEDs to excite those microspheres, respectively. Assessment of filters was also performed by imaging with no filter, red, green, and blue filters. ImageJ was used to separate the resulted images into their RGB (red, green, and blue) channels to determine the signal strength in each of the four setups (Figure 5d). Figure 5e shows that imaging the sample in bright mode and dark mode gave similar results, demonstrating the ability of the device to capture cell-sized beads. It was reported that the best contrast was attainable when the used emission filter, RGB channel, and microsphere had the same color. To evaluate the performance of setup in biological applications, cell counting and concentration determination ability of device was assessed using breast cancer cells that were cultured and stained with calcein in five different concentrations. The proposed device can measure the concentration of cancer cells with 10 µL of the sample, eliminating the need to obtain large samples from patients. The concentration of cells was determined accurately (0.95 linearity) with a detection limit of 680 cells per mL or 1 cell in 1.47 µL [51].

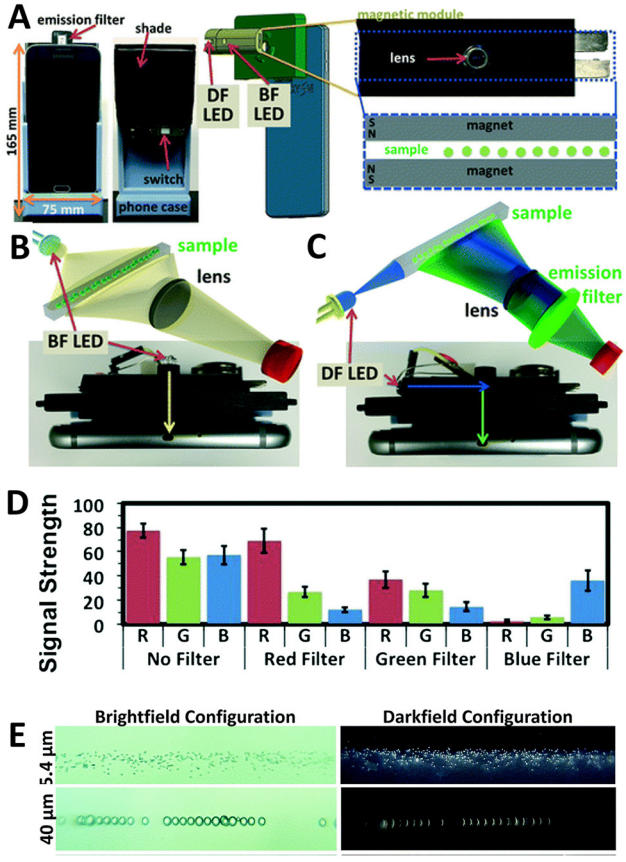

Figure 5: A fluorescence- and MagLev-based cytometry.
(a) Front and back views of the device. (b) (Top) schematic of brightfield imaging configuration and light path; (bottom) top view of the setup to display the simplified path of light. (c) (Top) schematic of darkfield imaging configuration for a sample excited by blue light and emitting green light; (bottom) top view of the setup to display a simplified path of light. (d) An example of fluorescence imaging results represented as signal strength, defined as the discrepancy between background pixel intensity and microsphere pixel intensity under the different physical filter. (e) Brightfield and darkfield images of 5.4 and 40 µm microspheres, demonstrating the capability of the proposed setup for imaging micron-sized particles (e.g., cells) [51].

3.2 Self-contained MagLev setups

Self-contained MagLev setups levitate, image the sample using a built-in camera, and analyze results from loaded samples, which is a low-cost (<100 $), user-friendly setup suitable for untrained users in the point of care. Although self-contained and smartphone-based MagLev devices share many advantages such as portability, user-friendliness, and low cost, self-contained MagLev platforms can offer further benefits over smartphone-based MagLevs. Heat and electromagnetic fields, generated by smartphone circuits, can conceivably affect the results of sensitive tests by altering the density of the paramagnetic medium. Additionally, in some cases where a smartphone with suitable processing power and a camera of good quality is not available, purchasing such a smartphone is required to be used with the attachment, drawing extra cost, even higher than the attachment itself which costs virtually $105 [51]. In contrast, a self-contained device does not require any additional cost, with an estimated cost of approximately $86 [52]. Furthermore, while smartphone attachable MagLev setups are designed and optimized for specific cellphones (e.g., specific focal length), different smartphones, with different camera properties, may be used on MagLev setup, particularly in deprived regions, posing challenges in standardization of setup for different smartphones.

A cost-effective (<100 $), self-contained setup was developed for the label-free detection of sickle cells in blood samples, in 15 min, using a drop of blood, and to analyze the results by an embedded Raspberry Pi computer running a Python script, with minimal need for user intervention (only reagent mixing) (Figure 6) [57]. The obtained blood was mixed with a paramagnetic medium (gadolinium solution and sodium metabisulfite) and loaded between two NdFeB permanent magnets (2 × 5 × 50 mm) with a 1.1 mm gap between magnets. The device used a 3D-printed case to hold the camera module, magnification lens, LED, and capillary tube. The levitation

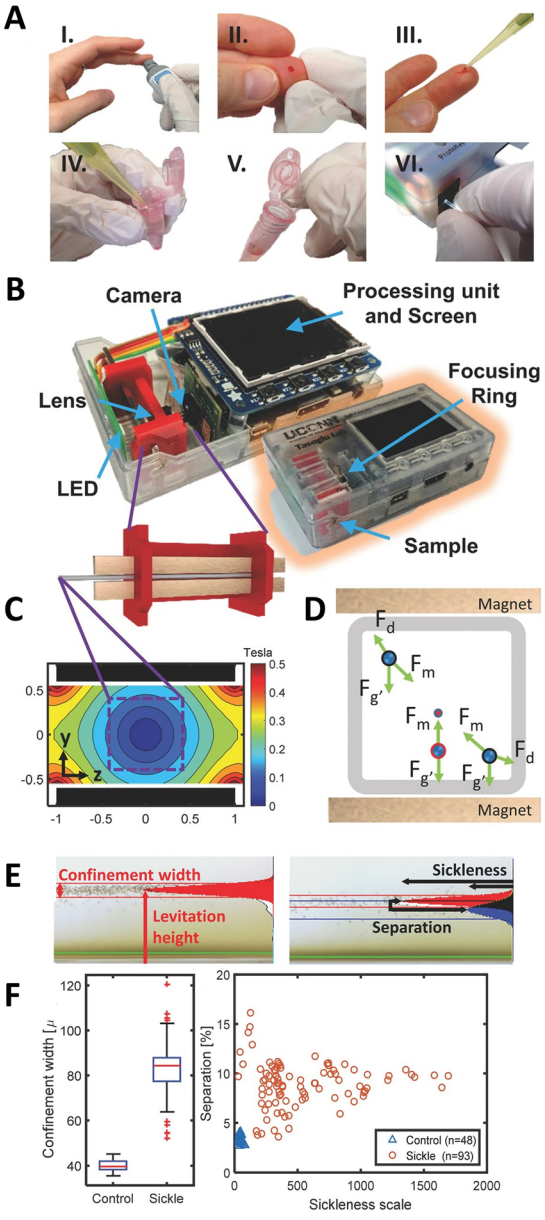

Figure 6: A self-contained MagLev setup for label-free sickle cell analysis.
(a) Sample preparation steps. (b) Inside of the device. Built-in camera, magnets, LED, and the lens were the main elements of the device. (c) Contour plot of the magnetic field in the cross-section of the capillary tube. (d) Different forces acting on a particle in the capillary tube. F_m: magnetic force, F_b: buoyant force, F_d: drag force, and $F_{g'}$: gravitational force. At equilibrium, F_d is zero, where F_m and F_d are equal and opposite. (e) (Left) confinement width and levitation height of RBCs in a magnetic field. (Right) separation (the difference between the average levitation heights normalized to the greater mean value), and sickleness (the ratio between the normal fit heights). (f) (Left) Experimental results for confinement width of SCD RBCs and control RBCs, defined as the total width of two Gaussian curves fit to pixel intensity gradient data. (Right) experimental results representing sickliness and separation percentage for the same SCD and control samples showed in the left figure [57].

height difference between polystyrene microspheres and RBCs was 35 and 110 μm for 100×10^{-3} mM and 25×10^{-3} mM concentration of the paramagnetic medium, respectively, pointing out a higher detection resolution to distinguish smaller density differences with a low concentration paramagnetic medium. The proposed device was able to effectively separate sickle cells from normal RBCs [57].

4 Conclusions and future perspectives

MagLev is an effective technique for the detection, separation, and quantification of objects based on their densities. Objects (e.g., solid particles, liquids, gels, and organic matter) can be levitated at a certain height (proportional to their density) in a paramagnetic medium, using magnets, as a result of an equilibrium of gravitational, buoyancy, and magnetic force acting on the object. Although large MagLev setups are in use widely for the analysis of food, water, polymer, chemical reactions, and forensic evidence, being costly and nonportable limit application of large MagLevs in remote, deprived regions. Smaller setups have been developed recently, using smaller magnets and low-cost optics, accompanied by imaging equipment (smartphone-based or self-contained cameras) to measure levitation height. Smaller MagLevs are cost-effective, portable, and less affected by surrounding magnetic fields. Smartphone-based MagLevs benefit from the ever-improving image acquisition and computational power of smartphones, attracting more attention recently. In order to provide an insight into the potency of smartphone-based MagLevs, in this review, we provided important design criteria of smartphone-based MagLev setups, along with end applications of smartphone-based MagLevs for biomedical applications, such as separation of different types of cells, detection of cancer cells, blood analysis, and diagnostic applications. Overall, smartphone-based MagLev platforms provide portability, ease of use, and low cost, making them useful for point-of-care diagnosis.

Dynamic range (which is important to separate samples with large density differences such as separating metal powders from polymer particles) and detection resolution (which is important to accurately distinguish subtle density differences between objects such as RBCs and WBCs) are two important parameters during the design process. A paramagnetic medium is one of the most influential elements of MagLev to achieve desired dynamic range and detection limit. A higher concentration of the paramagnetic medium results in a wider dynamic range,

whereas better detection resolution can be acquired by a lower concentration.

One of the limitations of MagLev setups is low throughput since, in most setups, a single container can be loaded between magnets each time. Integration of MagLev with multiplexed biomedical platforms [62, 63] and microfluidic chips [64, 65] enables the development of flow-assisted devices for continuous, real-time monitoring, and separation of materials. Another suggestion to extend the impact of MagLevs is developing data interpretation platforms. Although mobile software has been developed to analyze data, that software is confined to a particular particle that the software had been programmed for. Levitating objects other than predefined objects may challenge the performance of the device. Using machine learning techniques can empower MagLev setups to adapt themselves to new experiments without being programmed for that specific application [66, 67]. Moreover, optical magnification can be enhanced using smartphones with optical zoom and manual focusing options (e.g., LG V40 ThinQ which offers 2× optical zoom). Future studies can be focused to enable MagLevs to levitate and image submicron-sized particles (e.g., viruses), or to develop novel applications such as monitoring bone mass loss, that occur in astronauts who were in zero-gravity condition for a long period, since MagLev can simulate analogous condition (weightlessness) in the laboratory.

Acknowledgments: The authors have no other relevant affiliations or financial involvement with any organization or entity with a financial interest in or financial conflict with the subject matter or materials discussed in the manuscript apart from those disclosed.

Author contributions: All the authors have accepted responsibility for the entire content of this submitted manuscript and approved submission.

Research funding: This research was supported by the Tubitak 2232 International Fellowship for Outstanding Researchers Award (118C391), Alexander von Humboldt Research Fellowship for Experienced Researchers, Marie Skłodowska-Curie Individual Fellowship (101003361), and Royal Academy Newton-Katip Çelebi Transforming Systems Through Partnership Award (120N019). This work was partially supported by Science Academy's Young Scientist Awards Program (BAGEP), Outstanding Young Scientists Awards (GEBİP), and Bilim Kahramanlari Association The Young Scientist Award. Opinions, interpretations, conclusions, and recommendations are those of the author and are not necessarily endorsed by the TÜBİTAK.

Conflict of interest statement: The authors declare no conflicts of interest regarding this article.

References

[1] G. R. Philips, B. Gleich, G. A. Paredes-Juarez, A. Antonelli, M. Magnani, and J. W. Bulte, "Magnetic manipulation of blood conductivity with superparamagnetic iron oxide-loaded erythrocytes," *ACS Appl. Mater. Interfaces*, vol. 11, no. 12, pp. 11194–11201, 2019.

[2] S. L. Sparks, O. D. Brimhall, S. C. Peterson, and C. D. Baker, "Apparatus and methods for achieving urinary continence," Google Patents, 1989.

[3] V. P. Zharov, "Device and method for *in vivo* noninvasive magnetic manipulation of circulating objects in bioflows," Google Patents, 2015.

[4] S. Wang, S. Tasoglu, P. Z. Chen, et al, "Micro-a-fluidics ELISA for rapid CD4 cell count at the point-of-care," *Sci. Rep.*, vol. 4, no. 1, pp. 1–9, 2014.

[5] J. Haverkort, S. Kenjereš, and C. Kleijn, "Magnetic particle motion in a Poiseuille flow," *Phys. Rev. E*, vol. 80, no. 1, 2009, Art no. 016302.

[6] M. Takashima, "The stability of the modified plane Poiseuille flow in the presence of a transverse magnetic field," *Fluid Dynam. Res.*, vol. 17, no. 6, p. 293, 1996.

[7] J. M. Martel and M. Toner, "Inertial focusing in microfluidics," *Annu. Rev. Biomed. Eng.*, vol. 16, pp. 371–396, 2014.

[8] A. J. Chung, "A minireview on inertial microfluidics fundamentals: inertial particle focusing and secondary flow," *BioChip J.*, vol. 13, no. 1, pp. 53–63, 2019.

[9] J. Xie, P. Zhao, C. Zhang, J. Fu, and L.-S. Turng, "Current state of magnetic levitation and its applications in polymers: a review," *Sensor. Actuator. B Chem.*, vol. 333, 2021, Art no. 129533.

[10] F. Ozefe and A. A. Yildiz, "Smartphone-assisted hepatitis C detection assay based on magnetic levitation," *Analyst*, vol. 145, no. 17, pp. 5816–5825, 2020.

[11] A. R. Kose, B. Fischer, L. Mao, and H. Koser, "Label-free cellular manipulation and sorting via biocompatible ferrofluids," *Proc. Natl. Acad. Sci. Unit. States Am.*, vol. 106, no. 51, pp. 21478–21483, 2009.

[12] S. Tasoglu, J. A. Khoory, H. C. Tekin, et al, "Levitational image cytometry with temporal resolution," *Adv. Mater.*, vol. 27, no. 26, pp. 3901–3908, 2015.

[13] S. Tasoglu, C. H. Yu, V. Liaudanskaya, S. Guven, C. Migliaresi, and U. Demirci, "Magnetic levitational assembly for living material fabrication," *Adv. Healthc. Mater.*, vol. 4, no. 10, pp. 1469–1476, 2015.

[14] F. Ozefe and A. A. Yildiz, *Magnetic Levitation Based Applications in Bioscience. Magnetic Levitation*, London, UK, IntechOpen, 2020.

[15] S. Yaman and H. C. Tekin, "Magnetic susceptibility-based protein detection using magnetic levitation," *Anal. Chem.*, vol. 92, no. 18, pp. 12556–12563, 2020.

[16] H.-W. Lee, K.-C. Kim, and J. Lee, "Review of maglev train technologies," *IEEE Trans. Magn.*, vol. 42, no. 7, pp. 1917–1925, 2006.

[17] F. Werfel, U. Floegel-Delor, R. Rothfeld, et al, "Superconductor bearings, flywheels and transportation," *Supercond. Sci. Technol.*, vol. 25, no. 1, 2011, Art no. 014007.

[18] S. Ge, A. Nemiroski, K. A. Mirica, et al, "Magnetic levitation in chemistry, materials science, and biochemistry," *Angew. Chem. Int. Ed.*, vol. 59, no. 41, pp. 17810–17855, 2020.

[19] M. Anil-Inevi, E. Yilmaz, O. Sarigil, H. C. Tekin, and E. Ozcivici, *Single Cell Densitometry and Weightlessness Culture of Mesenchymal Stem Cells Using Magnetic Levitation. Stem Cell Nanotechnology*, Berlin, Germany, Springer, 2019, pp. 15–25.
[20] W. Braunbek, "Freischwebende Körper im elektrischen und magnetischen Feld," *Z. Phys.*, vol. 112, nos 11–12, pp. 753–763, 1939.
[21] R. D. Waldron, "Diamagnetic levitation using pyrolytic graphite," *Rev. Sci. Instrum.*, vol. 37, no. 1, pp. 29–35, 1966.
[22] I. Simon, A. G. Emslie, P. F. Strong, and R. K. McConnell Jr., "Sensitive tiltmeter utilizing a diamagnetic suspension," *Rev. Sci. Instrum.*, vol. 39, no. 11, pp. 1666–1671, 1968.
[23] I. Simon, "Diamagnetic accelerometer," Google Patents, 1969.
[24] U. Andres, *Magnetohydrodynamic & Magnetohydrostatic Methods of Mineral Separation*, Hoboken, New Jersey, USA, John Wiley & Sons, 1976.
[25] Y. Ikezoe, N. Hirota, J. Nakagawa, and K. Kitazawa, "Making water levitate," *Nature*, vol. 393, no. 6687, pp. 749–750, 1998.
[26] E. Beaugnon and R. Tournier, "Levitation of organic materials," *Nature*, vol. 349, no. 6309, p. 470, 1991.
[27] A. Catherall, L. Eaves, P. King, and S. Booth, "Floating gold in cryogenic oxygen," *Nature*, vol. 422, no. 6932, p. 579, 2003.
[28] M. Sagawa, S. Fujimura, N. Togawa, H. Yamamoto, and Y. Matsuura, "New material for permanent magnets on a base of Nd and Fe," *J. Appl. Phys.*, vol. 55, no. 6, pp. 2083–2087, 1984.
[29] J. J. Croat, J. F. Herbst, R. W. Lee, and F. E. Pinkerton, "Pr–Fe and Nd–Fe-based materials: a new class of high-performance permanent magnets," *J. Appl. Phys.*, vol. 55, no. 6, pp. 2078–2082, 1984.
[30] K. A. Mirica, F. Ilievski, A. K. Ellerbee, S. S. Shevkoplyas, and G. M. Whitesides, "Using magnetic levitation for three dimensional self-assembly," *Adv. Mater.*, vol. 23, no. 36, pp. 4134–4140, 2011.
[31] K. A. Mirica, S. S. Shevkoplyas, S. T. Phillips, M. Gupta, and G. M. Whitesides, "Measuring densities of solids and liquids using magnetic levitation: fundamentals," *J. Am. Chem. Soc.*, vol. 131, no. 29, pp. 10049–10058, 2009.
[32] K. A. Mirica, S. T. Phillips, C. R. Mace, and G. M. Whitesides, "Magnetic levitation in the analysis of foods and water," *J. Agric. Food Chem.*, vol. 58, no. 11, pp. 6565–6569, 2010.
[33] M. R. Lockett, K. A. Mirica, C. R. Mace, R. D. Blackledge, and G. M. Whitesides, "Analyzing forensic evidence based on density with magnetic levitation," *J. Forensic Sci.*, vol. 58, no. 1, pp. 40–45, 2013.
[34] K. A. Mirica, S. T. Phillips, S. S. Shevkoplyas, and G. M. Whitesides, "Using magnetic levitation to distinguish atomic-level differences in chemical composition of polymers, and to monitor chemical reactions on solid supports," *J. Am. Chem. Soc.*, vol. 130, no. 52, pp. 17678–17680, 2008.
[35] M. B. Atkinson, D. K. Bwambok, J. Chen, et al, "Using magnetic levitation to separate mixtures of crystal polymorphs," *Angew. Chem.*, vol. 125, no. 39, pp. 10398–10401, 2013.
[36] A. Winkleman, R. Perez-Castillejos, K. L. Gudiksen, S. T. Phillips, M. Prentiss, and G. M. Whitesides, "Density-based diamagnetic separation: devices for detecting binding events and for collecting unlabeled diamagnetic particles in paramagnetic solutions," *Anal. Chem.*, vol. 79, no. 17, pp. 6542–6550, 2007.
[37] A. B. Subramaniam, M. Gonidec, N. D. Shapiro, K. M. Kresse, and G. M. Whitesides, "Metal-amplified density assays,(MADAs), including a density-linked immunosorbent assay (DeLISA)," *Lab Chip*, vol. 15, no. 4, pp. 1009–1022, 2015.
[38] S. Tasoglu, D. Kavaz, U. A. Gurkan, et al, "Paramagnetic levitational assembly of hydrogels," *Adv. Mater.*, vol. 25, no. 8, pp. 1137–1143, 2013.
[39] S. Knowlton, C. H. Yu, N. Jain, I. C. Ghiran, and S. Tasoglu, "Smart-phone based magnetic levitation for measuring densities," *PloS One*, vol. 10, no. 8, 2015, Art no. e0134400.
[40] C. J. Luby, B. P. Coughlin, and C. R. Mace, "Enrichment and recovery of mammalian cells from contaminated cultures using aqueous two-phase systems," *Anal. Chem.*, vol. 90, no. 3, pp. 2103–2110, 2018.
[41] A. A. Kumar, M. R. Patton, J. W. Hennek, et al, "Density-based separation in multiphase systems provides a simple method to identify sickle cell disease," *Proc. Natl. Acad. Sci. Unit. States Am.*, vol. 111, no. 41, pp. 14864–14869, 2014.
[42] T. Kenner, "The measurement of blood density and its meaning," *Basic Res. Cardiol.*, vol. 84, no. 2, pp. 111–124, 1989.
[43] R. C. Miller, E. Brindle, D. J. Holman, et al, "Comparison of specific gravity and creatinine for normalizing urinary reproductive hormone concentrations," *Clin. Chem.*, vol. 50, no. 5, pp. 924–932, 2004.
[44] S. M. Knowlton, I. Sencan, Y. Aytar, et al, "Sickle cell detection using a smartphone," *Sci. Rep.*, vol. 5, no. 1, pp. 1–11, 2015.
[45] R. Amin, S. Knowlton, J. Dupont, et al, "3D-printed smartphone-based device for label-free cell separation," *J. 3D Print. Med.*, vol. 1, no. 3, pp. 155–164, 2017.
[46] M. Baday, S. Calamak, N. G. Durmus, R. W. Davis, L. M. Steinmetz, and U. Demirci, "Integrating cell phone imaging with magnetic levitation (i-LEV) for label-free blood analysis at the point-of-living," *Small*, vol. 12, no. 9, pp. 1222–1229, 2016.
[47] E. J. Felton, A. Velasquez, S. Lu, et al, "Detection and quantification of subtle changes in red blood cell density using a cell phone," *Lab Chip*, vol. 16, no. 17, pp. 3286–3295, 2016.
[48] R. Amin, S. Knowlton, B. Yenilmez, A. Hart, A. Joshi, and S. Tasoglu, "Smart-phone attachable, flow-assisted magnetic focusing device," *RSC Adv.*, vol. 6, no. 96, pp. 93922–93931, 2016.
[49] H-S. Han and D-S. Kim, *Magnetic Levitation*, Netherlands, Springer, 2016.
[50] C. Zhang, P. Zhao, F. Gu, et al, "Single-ring magnetic levitation configuration for object manipulation and density-based measurement," *Anal. Chem.*, vol. 90, no. 15, pp. 9226–9233, 2018.
[51] S. Knowlton, A. Joshi, P. Syrrist, A. F. Coskun, and S. Tasoglu, "3D-printed smartphone-based point of care tool for fluorescence-and magnetophoresis-based cytometry," *Lab Chip*, vol. 17, no. 16, pp. 2839–2851, 2017.
[52] B. Yenilmez, S. Knowlton, and S. Tasoglu, "Self-contained handheld magnetic platform for point of care cytometry in biological samples," *Adv. Mater. Technol.*, vol. 1, no. 9, 2016, Art no. 1600144.
[53] D. K. Bwambok, M. M. Thuo, M. B. Atkinson, K. A. Mirica, N. D. Shapiro, and G. M. Whitesides, "Paramagnetic ionic liquids for measurements of density using magnetic levitation," *Anal. Chem.*, vol. 85, no. 17, pp. 8442–8447, 2013.
[54] N. G. Durmus, H. C. Tekin, S. Guven, et al, "Magnetic levitation of single cells," *Proc. Natl. Acad. Sci. Unit. States Am.*, vol. 112, no. 28, pp. E3661–E3668, 2015.

[55] A. Winkleman, K. L. Gudiksen, D. Ryan, G. M. Whitesides, D. Greenfield, and M. Prentiss, "A magnetic trap for living cells suspended in a paramagnetic buffer," *Appl. Phys. Lett.*, vol. 85, no. 12, pp. 2411–2413, 2004.

[56] N. D. Shapiro, K. A. Mirica, S. Soh, et al, "Measuring binding of protein to gel-bound ligands using magnetic levitation," *J. Am. Chem. Soc.*, vol. 134, no. 12, pp. 5637–5646, 2012.

[57] B. Yenilmez, S. Knowlton, C. H. Yu, M. M. Heeney, and S. Tasoglu, "Label-free sickle cell disease diagnosis using a low-cost, handheld platform," *Adv. Mater. Technol.*, vol. 1, no. 5, 2016, Art no. 1600100.

[58] N. D. Shapiro, S. Soh, K. A. Mirica, and G. M. Whitesides, "Magnetic levitation as a platform for competitive protein–ligand binding assays," *Anal. Chem.*, vol. 84, no. 14, pp. 6166–6172, 2012.

[59] S. R. Dabbagh, M. R. Sarabi, R. Rahbarghazi, E. Sokullu, A. K. Yetisen, and S. Tasoglu, "3D-Printed Microneedles in Biomedical Applications," *iScience*, vol. 24, 2020, Art no. 102012.

[60] R. Amin, S. Knowlton, A. Hart, et al, "3D-printed microfluidic devices," *Biofabrication*, vol. 8, no. 2, 2016, Art no. 022001.

[61] M. S. Andersen, E. Howard, S. Lu, et al, "Detection of membrane-bound and soluble antigens by magnetic levitation," *Lab Chip*, vol. 17, no. 20, pp. 3462–3473, 2017.

[62] M. R. Sarabi, N. Jiang, E. Ozturk, A. K. Yetisen, and S. Tasoglu, "Biomedical optical fibers," *Lab Chip*, vol. 21, no. 4, pp. 627–640, 2021.

[63] F. Ghaderinezhad, H. C. Koydemir, D. Tseng, et al, "Sensing of electrolytes in urine using a miniaturized paper-based device," *Sci. Rep.*, vol. 10, no. 1, pp. 1–9, 2020.

[64] S. Knowlton, A. Joshi, B. Yenilmez, et al, "Advancing cancer research using bioprinting for tumor-on-a-chip platforms," *Int. J. Bioprint.*, vol. 2, no. 2, pp. 3–8, 2016.

[65] Z. Luo, S. Güven, I. Gozen, et al, "Deformation of a single mouse oocyte in a constricted microfluidic channel," *Microfluid. Nanofluidics*, vol. 19, no. 4, pp. 883–890, 2015.

[66] S. R. Dabbagh, F. Rabbi, Z. Doğan, A. K. Yetisen, and S. Tasoglu, "Machine learning-enabled multiplexed microfluidic sensors," *Biomicrofluidics*, vol. 14, no. 6, 2020, Art no. 061506.

[67] J. Riordon, D. Sovilj, S. Sanner, D. Sinton, and E. W. Young, "Deep learning with microfluidics for biotechnology," *Trends Biotechnol.*, vol. 37, no. 3, pp. 310–324, 2019.